

THE STELLAR X-RAY POLARIMETER FOR THE SPECTRUM-X-GAMMA MISSION

P. KAARET, R. NOVICK, C. MARTIN, P. SHAW,
J.R. FLEISCHMAN, T. HAMILTON

Columbia Astrophysics Laboratory, Columbia University, New York, NY

R. SUNYAEV, I. LAPSHOV

Space Research Institute of the USSR Academy of Sciences, USSR

E. SILVER, K. ZIOCK

Lawrence Livermore National Laboratory, USA

M. WEISSKOPF, R. ELSNER, B. RAMSEY

NASA/Marshall Space Flight Center, Huntsville, AL

G. CHANAN

University of California, Irvine, CA

G. MANZO, S. GIARRUSSO, A. SANTANGELO

IFCAI/CNR, Palermo, Italy

E. COSTA, L. PIRO

IAS/CNR, Frascati, Italy

G. FRASER, J.F. PEARSON, J.E. LEES

University of Leicester, UK

and

G.C. PEROLA, E. MASSARO, G. MATT

University of Rome, Italy

Abstract. We describe an X-ray polarimeter which will be flown on the SPECTRUM-X-Gamma mission. The instrument exploits three distinct physical processes to measure polarization: Bragg reflection from a graphite crystal, Thomson scattering from a metallic lithium target, and photoemission from a Cesium Iodide photocathode. These three processes allow polarization measurements over an energy band of 0.3 keV to 12 keV. The polarimeter will make possible sensitive measurements of several hundred known X-ray sources. X-ray polarization measurements will allow us to constrain the geometry of gas flow in X-ray binaries, identify nonthermal emission in supernova remnants, test current models for X-ray emission in radio pulsars, determine the radiation mechanisms in active galactic nuclei, and search for inertial frame dragging (Lense-Thirring effect) around the putative black hole in Cygnus X-1.

1. Introduction

The high resolution instruments available on the next generation of X-ray observatories will allow X-ray observations with angular, energy, and timing resolution comparable to that obtained in optical astronomy. To complete our knowledge of the X-radiation from astrophysical sources it will be necessary to measure the remaining parameter of the radiation, the polarization. The Stellar X-Ray Polarimeter

Y. Kondo (ed.), Observatories in Earth Orbit and Beyond, 443-449.

© 1990 Kluwer Academic Publishers. Printed in The Netherlands.

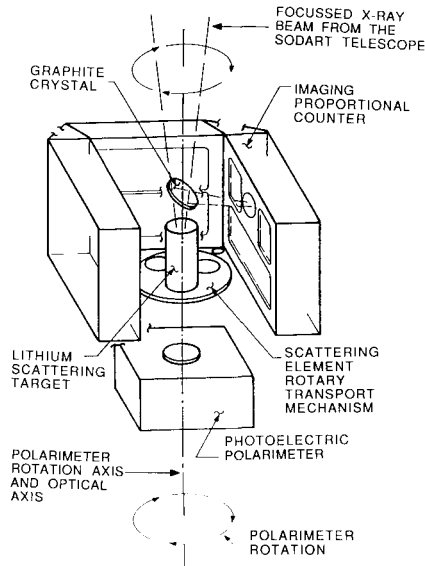


Fig. 1. Elements of the SXP. When the scattering polarimeter is in use, the graphite crystal and the lithium target are placed on the optical axis of the SODART telescope (shown as a dashed line). The scattered X-rays are detected by four imaging proportional counters, (one of the four is not shown). When the photoelectric polarimeter is in use, the crystal and target are moved off the optical axis so that X-rays may pass through to the photoelectric polarimeter. The entire assembly rotates about the telescope optical axis with a period of approximately ten minutes.

(SXP) is the only orbiting X-ray polarimeter currently scheduled to fly (Kaaret *et al.* 1989). It will be the only instrument capable of extending X-ray observations to the full parameter space of the radiation. The SXP, which will be flown at the focus of one of the SODART telescopes on the SPECTRUM-X-Gamma mission (R.A. Sunyaev 1990), will increase the number of sources in which X-ray polarization is detectable from one supernova remnant at present (Novick *et al.* 1972) to several hundred objects including X-ray binaries, isolated radio pulsars, additional supernova remnants, black holes, and active galactic nuclei.

In this paper, we first review the techniques used to make polarization measurements. Then we describe the design of our instrument, highlighting the features necessary to obtain good polarization sensitivity. Finally, we discuss a number of polarimetric observations, made possible by the SXP, which would provide important new information about a variety of astrophysical sources.

2. Instrument Concept

The SXP exploits the polarization dependence of Bragg reflection from a graphite crystal, of Thomson scattering from a metallic lithium target, and of photoemission

from a Cesium Iodide photocathode. The instrument is divided into two parts, as shown in Figure 1. One part, the scattering polarimeter, contains the Bragg crystal, the Thomson scattering target, and four imaging proportional counters (IPC's). The other part, the photoelectric polarimeter (PEP), contains a CsI photocathode and an electron detector. Both parts are mounted on a platform which rotates with a period of approximately 10 minutes.

The graphite crystal and the lithium scattering target are mounted on a mechanism which allows them to be either positioned on the optical axis or removed from the optical path. When these two elements are aligned with the optical axis of the telescope, they scatter the incident X-rays into the surrounding IPC's. When they are off the optical axis, the X-rays from the telescope pass into the photoelectric polarimeter. The movable wheel on which the lithium target is mounted has three positions. One position holds the lithium target. The other positions contain filters for use with the photoelectric polarimeter. Use of two filters gives the PEP two-color energy resolution.

The signature of polarization for any of the three polarization elements is a count rate which varies at twice the rotation frequency of the polarimeter detector assembly. To detect polarization, we must observe the sinusoidal variation in count rate superimposed over the average counting rate. The average counting rate has two components. One component is the background counting rate. The other component arises because the crystal and the scattering target are not perfect polarization analysers. The magnitude of modulation for 100% polarized X-rays and no background is referred to as the modulation factor, μ , and is defined as the ratio of the amplitudes of the modulated and unmodulated components of the signal. We define the minimum detectable polarization (MDP) of a polarimeter element as the minimum level of polarization which it can detect at a 99% statistical confidence level for a given observation. We can relate the MDP to the source counting rate r , the length of the observation T , the modulation factor μ , and background counting rate b using Poisson statistics,

$$\text{MDP} = \frac{4.29}{\mu r} \sqrt{\frac{r + b}{T}}$$

To obtain the best polarization sensitivity we must design the polarimeter with the maximum possible modulation factor and counting rate and the minimum possible background rate. We discuss the design of each polarimeter element below.

The scattering polarimeter contains a graphite crystal mounted above a cylinder of lithium. A graphite crystal oriented at 45° to an incoming x-ray beam will reflect only those X-rays with energies satisfying the Bragg condition and electric vectors lying in the plane of the crystal. If the incident beam is polarized, the intensity of the reflected beam will be modulated at twice the rotation frequency of the polarimeter. The polarization dependence of the Thomson cross-section for scattering of X-rays from electrons gives rise to a sinusoidal dependence in the azimuthal angular distribution. The count rate from a small fixed area of an IPC will vary at twice the rotation frequency of the platform. We have found that a very thin graphite crystal can be used to efficiently reflect X-rays at the first order and second order Bragg peaks, while allowing the X-rays that do not satisfy the Bragg condition

to pass through the crystal with only moderate attenuation (Silver *et al.* 1989). Placing the graphite crystal above the lithium target permits us to obtain data from both polarization elements simultaneously. The graphite crystal and lithium target are surrounded by four imaging proportional counters that are used to detect the reflected or scattered X-rays.

The key characteristic in selecting a Bragg crystal is its reflectivity. Higher reflectivities lead to higher counting rates and increased polarization sensitivity. We have chosen graphite crystals because they provide the highest obtainable reflectivity in the energy range of interest. The graphite crystal is sensitive in very narrow energy bands (bandwidth of a few tenths of a keV for the converging X-rays from the SODART telescope) centered on the 45° Bragg reflection peaks at 2.6 and 5.2 keV. The modulation factor for the crystal is above 99%.

The scattering target is a cylinder of metallic lithium 30 mm in diameter and 50 mm long. Lithium is used because it has the highest ratio of Thomson to photoelectric cross-sections of any workable material. The target is sufficiently long to ensure that more than half the X-rays interact in the target at energies below 15 keV. This part of the instrument provides broad band energy coverage extending from 5 keV, limited by photoelectric absorption in lithium, to about 12 keV, limited by the telescope optics. Because the photon energy changes only slightly during scattering, it is possible to measure polarization versus energy with an energy resolution determined by the proportional counters. The modulation factor for the lithium scattering target, used with an imaging X-ray detector, is 81% (Weisskopf *et al.* 1989).

To detect the scattered X-rays, we use four imaging proportional counters forming a box surrounding the scattering elements. The detectors are sensitive over the scattering polarimeter energy band of 2 to 15 keV. The counters should have an energy resolution of 18% and a position resolution of 1 mm at 6 keV. We have chosen to use imaging detectors because position sensing: increases the modulation factor for lithium scattered X-rays from 28% to 81%, permits us to correct for nonuniformities in the detector response, and allows us to continuously measure the background and its possible spurious polarization signature. The position resolution chosen is a small fraction of the diameter of the SODART telescope blur circle. Because the X-rays from the telescope are either reflected or scattered before they are detected, the flux of X-rays reaching the detector is greatly reduced and low background rates are essential in measuring the polarization of weak sources. We believe we can achieve a background counting rate of less than 10^{-3} counts/sec·cm²·keV by the use of anticoincidence and pulse shape discrimination background rejection techniques together with careful choice of materials to reduce the inherent and induced radioactivity in the detector body.

The photoelectric polarimeter (PEP) exploits the recently discovered polarization dependence of soft X-ray photoemission. This effect was first reported in the x-ray band by Fraser *et al.* (1988). Further studies of the effect have been performed at Columbia and Leicester (Heckler *et al.* 1989, Fraser *et al.* 1989). A polarization dependence is observed in both the total photocurrent and in the number of photoelectrons produced for each X-ray when an X-ray beam is incident on a photocathode at a very shallow grazing angle (on the order of 10°). When the photocathode is

rotated around the axis of the incident X-rays, the photoelectron yield is modulated at twice the rotation frequency. The modulation factor of the polarization signal depends on the energy and angle of incidence of the X-rays and has a maximum magnitude of roughly 30% for 1 keV X-rays at a grazing angle of 8° .

The polarization sensitive element of the PEP will be a microchannel plate (MCP) with square pores. We use a square-pore MCP because the magnitude of the polarization modulated signal depends very sensitively on the grazing angle between the incident X-rays and the photocathode surface. By using a square-pore MCP we can maintain a constant grazing angle over the entire surface of the MCP. Beneath the square-pore MCP there will be a stack of conventional MCP's. The square-pore MCP is operated at low gain to preserve information on the number of photoelectrons produced. The conventional MCP are used to amplify the signal. The electrons will be collected on a wedge and strip anode to give position information. Imaging will improve the performance of the system, allowing us to reduce the background via spatial cuts and permitting us to continually monitor the background. The energy range of the polarimeter is determined at the high end by the quantum efficiency of CsI, the cutoff is about 3 keV, and at the low end of our choice of filters. A thin (0.5 micron) beryllium filter will be permanently mounted over the detector. This gives a low energy cutoff near 0.3 keV. We will have another filter with a higher low energy cutoff mounted on a movable wheel. This will give the photoelectric polarimeter two-color energy resolution.

The photoelectric polarimeter offers a great increase in polarization sensitivity over the scattering polarimeter, due to its vastly superior quantum efficiency. This increase is slightly tempered because the modulation factor of the photoelectric process is lower than for the scattering processes. The net increase in polarization sensitivity, relative to the Bragg crystal, is almost a factor of ten. For observations of sources with fluxes of a few milliCrabs, the PEP can achieve a given level of polarization sensitivity in 1/30th the time required by the Bragg crystal polarimeter.

3. Observations

X-rays are produced with significant polarization when the X-ray emission mechanism is non-thermal or when the X-rays are scattered by electrons in anisotropic geometries. The degree and position angle of the polarization depend on the geometry of the source, thus polarization measurements provide information on the geometry of the X-ray emitting region. In the following, we discuss a polarimetric observations of a few of the classes of objects about which X-ray polarimetry should provide significant new information.

The polarization of X-rays from accreting pulsars is expected to be quite large, near 100% in certain geometries (Gnedin and Sunyaev 1974). Using radiative transfer models it is possible to predict the polarization, and its energy and pulse phase dependence, for pencil and fan beam accretion geometries (Rees 1975, Meszaros *et al.* 1988). Using the scattering polarimeter of the SXP we will be able to measure the X-ray polarization of Her X-1 in five pulse phase bins and three energy bins with an average MDP of 1.6% in each bin in a 7×10^5 second observation. This will definitively distinguish between the pencil and fan beam geometries. In addition,

we will be able to measure the average polarization of a number of other X-ray binaries (Cen X-3, GX1+4, 4U1626-67, ...) to a level of a few percent in individual 10^5 second observations.

Perhaps the most definitive test for the presence of a black hole is its X-ray polarization signature. The gravitational field near a massive rotating body causes inertial frames near the body to rotate with respect to a distant observer (the Lense-Thirring effect). If a black hole is surrounded by a thin accretion disk, the observed X-rays will be linearly polarized due to scattering in the disk, (Eardley *et al.* 1978; Lightman and Shapiro 1976; Gnedin and Silat'ev 1978). Because the gravitation field near the black hole is stronger, higher energy X-rays are produced closer to the black hole. The degree of rotation due to the Lense-Thirring effect also increases closer to the hole. Therefore, there is an indirect correlation between the energy of an X-ray and degree of rotation of its polarization vector. Observation of a rotation of X-ray polarization versus energy, would give a clear indication of the presence of a black hole and also probe an untested aspect of general relativity. In a 7×10^5 second observation of Cyg X-1 in its high state, the SXRPP, using both the scattering and photoelectric polarimeters, will measure the polarization to better than 0.3% across an energy band from 0.3 to 10 keV and will be able to detect a 10° rotation of the polarization vector across the same energy range. This is sufficient to refute or confirm the theoretically predicted polarization signature (Connors, Piran, and Stark 1980).

The X-ray spectra and total luminosity of active galactic nuclei are not sufficient to uniquely identify the X-ray emission mechanism. X-ray polarization measurements will provide valuable information on the emission process and on the geometry of the central power source. If the emission is due to synchrotron radiation then high X-ray polarization is expected (Ginzburg and Syrovatskii 1965). If the emission is by inverse Compton scattering and the geometry is not spherically symmetric then measurable polarization will be produced (Katz 1976; Shapiro, Lightman, and Eardley 1976; Pozdnyakov, Sobol, and Sunyaev 1976). If the main energy source is thermal, polarization can still arise from electron scattering in the accretion disk around the source (Angel 1969; Basko, Sunyaev, and Titarchuk 1974; Rees 1975; Matt 1989). The scattering polarimeter can provide a measurement of polarization for energies at and above the iron K fluorescence for a few of the brighter AGN. This will allow us to identify reprocessed emission from the accretion disk. However, the main observations of AGN will be done with the PEP. With the high sensitivity of the PEP, the SXRPP will be able to measure the polarization, in an energy band from 0.3 to 3 keV, of about a dozen AGN to a level of 3% in individual 10^5 second observations.

Acknowledgements

We wish to thank Richard Spalding, Joseph Chavez, Robert Woods, Patricia Newman, James Daniels, Gary Ahasten, George Peterson, Ronald Akau, and Kate Scurry of the Sandia National Laboratories, and Irwin Rochwarger, Eric Jauch, Alan Goodman, Robert Watkins, and Paul Okun of Columbia University for their numerous contributions to this project. This work was supported by NASA grant

NAG 5-618. This is contribution number 424 of the Columbia Astrophysics Laboratory.

References

- Angel, J.R.P.: 1969, *Ap. J.* **158**, 219
- Basko, M.M., R.A. Sunyaev, and I.G. Titarchuk: 1974, *Astron. Ap.* **31**, 749
- Connors, P.A., T. Piran, and R.F. Stark: 1980, *Ap. J.* **235**, 224–244
- Eardley, D.M. *et al.*: 1978, *Comments on Astrophysics* **8**, 151
- Fraser, G.W., J.F. Pearson, J.E. Lees and W.B. Feller: 1988, *Proc. SPIE* **982**, 98–107
- Fraser, G.W. *et al.*: 1989, *Proc. SPIE* **1160**, 568–579
- Ginzburg, V.I., and S.I. Syrovatskii: 1965, *Ann. Rev. Ast. Ap.* **3**, 297
- Gnedin, Yu.N., and R.A. Sunyaev: 1974, *Astron. and Astrophys* **36**, 379–394
- Gnedin, Yu.N., and N.A. Silat'ev: 1978, *Sov. Astron.* **22**, 325
- Heckler, A., A. Blaer, P. Kaaret, and R. Novick: 1989, *Proc. SPIE* **1160**, 580–586
- Kaaret, P. *et al.*: 1989, *Proc. SPIE* **1160**, 587–598
- Katz, J.I.: 1973, *Nature* **246**, 87
- Lightman, A.P., and S.L. Shapiro: 1976, *Ap. J.* **203**, 701
- Matt G., E. Costa, G.C. Perola, and L. Piro: 1989, *Proc. 23rd ESLAB Symposium*
- Meszaros, P. *et al.*: 1988, *Ap. J.* **324**, 1056–1067
- Novick, R., *et al.*: 1972, *Ap. J.* **174**, L1–L8
- Pozdynakov, L.A., I.M. Sobol, and R.A. Sunyaev: 1976, *Sov. Astron. Lett* **2**, 55
- Rees, M.J.: 1975, *M.N.R.A.S.* **171**, 457
- Shapiro, S.L., A.P. Lightman, and D.M. Eardley: 1976, *Ap. J.* **204**, 187
- Silver, E.H., *et al.*: 1989, *Proc. SPIE* **1160**, 598–609
- Sunyaev, R.A., 1990, these proceedings
- Weisskopf, M.C. *et al.*: 1989, *Proc. SPIE* **1159**, 607–616